GaN HEMT trap-induced variability through concurrent noise and AC TCAD modelling

GaN HEMT trap-induced variability through concurrent noise and AC TCAD modelling

Eva Catoggio
DET Department
Politecnico di Torino
Torino, Italy
eva.catoggio@polito.it

Simona Donati Guerrieri
DET Department
Politecnico di Torino
Torino, Italy
simona.donati@polito.it

Fabrizio Bonani
DET Department
Politecnico di Torino
Torino, Italy
fabrizio.bonani@polito.it

***Abstract*—In this work we exploit an in-house code implementing the drift-diffusion model coupled to trap rate equations to investigate the effect of Fe-induced buffer traps on the noise and AC behavior of GaN HEMTs. The model, exploiting a Green's function approach, shows that the noise frequency behavior is mainly due the trap equation Green's Functions. Local noise sources are concentrated below the channel, extending in the buffer region. Statistical variation/uncertainty in the trap parameters significantly affect both the low frequency noise spectra and the Y parameters. We show a significant correlation between these quantities. The proposed analysis demonstrates that the developed code represents a promising tool to assist both the identification of trap parameters from experimental data, and to extract compact device models.**

***Index Terms*—Trap Noise, GaN HEMTs, TCAD noise models, TCAD small-signal analysis**

I. Introduction

GaN HEMT technology is very appealing for high power and high frequency applications thanks to the excellent GaN material properties, e.g., wide bandgap, high electron mobility and good thermal stability [1]. Nonetheless, trapping mechanisms occurring inside the device may lead to performance degradation and reliability problems, making the investigation of trap dynamics necessary to limit these detrimental effects [2]. Traps induce important frequency dispersion in the device dynamic behavior, e.g., the gate and drain lag [3], [4] or the low frequency dispersion of the device Y parameters [5], [6]. Furthermore, traps can also undergo statistical fluctuations in terms of, e.g., trap concentration and energy, which further affect the device behavior and the overall terminal characteristics. Trap characterization can be, thus, helpful to identify their localization inside the device (buffer, interface, surface, ...) and to predict the spread at the output terminals. In this scenario, TCAD analysis can be necessary to complement measured data and develop consistent large-signal models. Furthermore, variability assessment directly yields important information to complement design-oriented compact device models.

Here, we investigate the effect of Fe-induced buffer traps on the small-signal AC parameters and linear noise spectrum in a GaN-based HEMT, demonstrating a strong correlation between these two quantities and the presence of a non trivial frequency trend with multiple time constants, despite the presence of a single trap.

II. Trap model implementation

In this work, we exploit an in-house TCAD simulator implementing explicitly trap rate equations (TRE) coupled to the drift-diffusion (DD) model [7]. For each trap, the TRE reads:

$$\frac{\partial n_T}{\partial t} = (R_n - G_n) - (R_p - G_p) \tag{1}$$

where n_T is the concentration of the occupied trap. The charge density in the Poisson equation is modified adding the trap charge as $(-n_T + \delta_T N_T)$, where N_T is the trap concentration and $\delta_T = 0$ for acceptor-like, or $\delta_T = 1$ for donor traps. Traps are treated according to the standard Shockley-Read-Hall theory, described by the cross sections σ_n and σ_p the trap energy E_T. In the current TCAD implementation [7], traps are assumed non interacting in terms of energy transitions and the trap rate equations are local. The extension to locally interacting traps is straightforward [8].

The physical model is solved in the frequency domain through the Harmonic Balance (HB) technique, allowing for the investigation of device behavior in small-signal (linear) and large-signal (nonlinear) periodic regime in a unique framework. In particular, the in-house code implements the Large-Signal (LS) and Small-Signal Large-Signal (SSLS) algorithms to extract the device Green's Function (GF), which, in turn, allow for a numerically efficient concurrent statistical (variability [9]) and noise analyses [10].

According to the GF approach, the current noise spectrum at terminals i and j due to trap dynamics can be extracted, as a function of the frequency f, using the spatial convolution (Ω is the device volume):

$$\mathbf{S}_I^{(i,j)}(f) = \sum_{\alpha,\beta} \int_\Omega \mathbf{G}_\alpha^{(i)}(\mathbf{r}, f)\mathbf{K}_{\alpha,\beta}(\mathbf{r})\mathbf{G}_\beta^{(j)}(\mathbf{r}, f)^\dagger \mathrm{d}\mathbf{r} \tag{2}$$

where $\mathbf{G}_\alpha^{(i)}(\mathbf{r}, f)$ is the GF of each model equation ($\alpha = \varphi$ Poisson, $\alpha = n, p$ electron/hole continuity equation, $\alpha = n_T$ trap rate equation) and observation at terminal i. The kernels $\mathbf{K}_{n,n} = \mathbf{K}_{n,n_T} = 2(R_n + G_n)$ (similar for holes) and $\mathbf{K}_{n_T,n_T} = 2(R_n + G_n) + 2(R_p + G_p)$ are the *microscopic noise sources*, i.e., the spectra of the local stochastic sources in each model equation. For trap noise, we exploit the rigorous white sources, contrary to the approximate equivalent

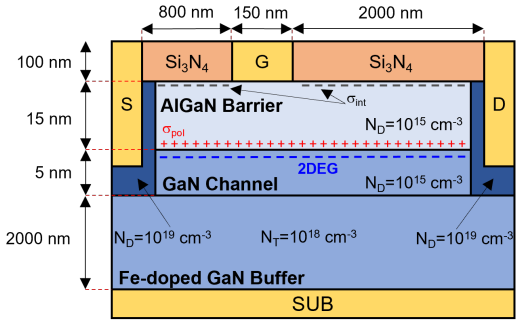

Fig. 1: Simulated HEMT structure. The device periphery is 1 cm.

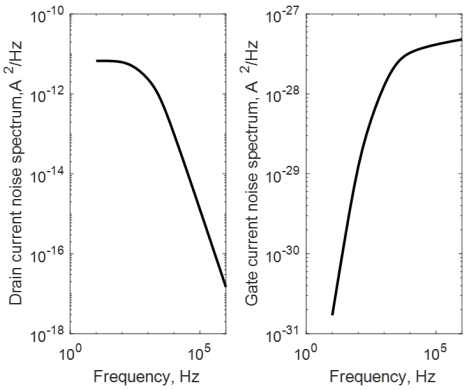

Fig. 2: Drain and gate trap noise spectra vs. frequency.

Lorentzian-like sources [8] sometimes found in the literature. The integrand function in (2) is known as the *local noise source* (*LNS*).

III. Case Study

We simulate the 150 nm gate length HEMT shown in Fig. 1 (left), made of an AlGaN barrier with 25% Al mole fraction, and of a GaN layer with a residual donor doping of 10^{15} cm^{-3}. The channel region, 5 nm thick, is placed above a 2 μm deep buffer characterized by a Fe-induced deep acceptor-like traps, assumed with uniform concentration $N_T = 10^{18}$ cm^{-3}, nominal energy 0.45 eV below E_C and $\sigma_n = \sigma_p = 3 \times 10^{-16}$ cm^{-3} (see [7] for further model details). DC analysis shows that the device threshold is -2.5 V. We investigate AC parameters and noise at $V_G = -2.2$ V and $V_D = 10$ V, a bias point suited for class AB power amplifier design. In this stationary condition, Fig. 2 shows the simulated drain and gate noise spectrum. Noticeably, the low-frequency (Lorentzian-like) noise trend is correctly recovered starting from white sources by the frequency dependent GFs.

The local noise source is then analyzed, to investigate how traps located deep in the substrate induce noise at the device terminals. Referring back to (2), we find that the dominant contribution to the overall noise always stems from the microscopic noise sources of the trap equations i.e., $\alpha = \beta = n_T$. Focusing first on the drain noise spectrum at $f = 100$ Hz, below the frequency cut-off, Fig. 3 shows the trap microscopic noise source. Since it depends on the recombination rates, its portrait closely resembles the occupied trap concentration, extending in the area immediately below the channel, located at $y = -0.115$ μm, and presenting a notch towards the drain contact (see [7] for further details). Fig. 4 shows $\mathbf{G}_{n_T}^{(D)}(\mathbf{r}, f)$:

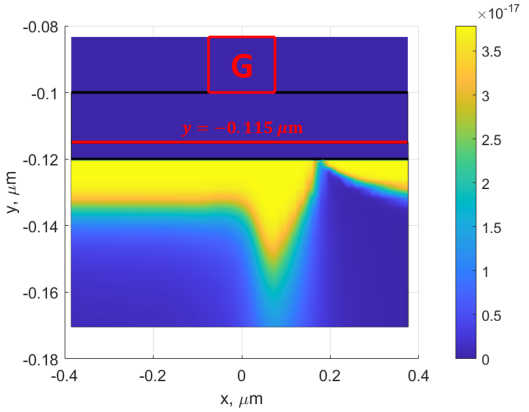

Fig. 3: Microscopic noise source for the drain current noise at $f = 100$ Hz. The red solid line represents the channel located at $y = -0.115$ μm.

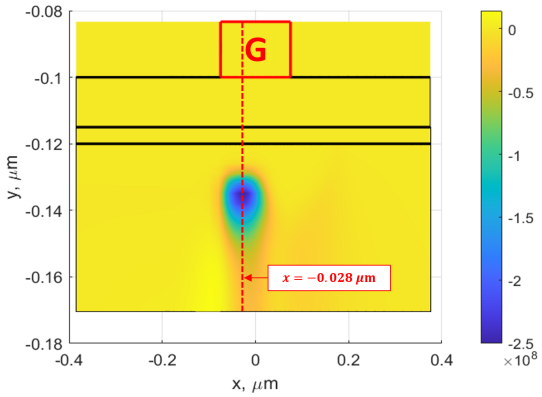

(a) Real part.

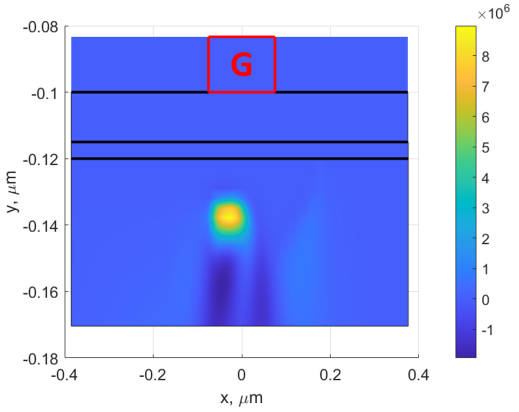

(b) Imaginary part.

Fig. 4: $\mathbf{G}_{n_T}^{(D)}(\mathbf{r}, f)$ at $f = 100$ Hz.

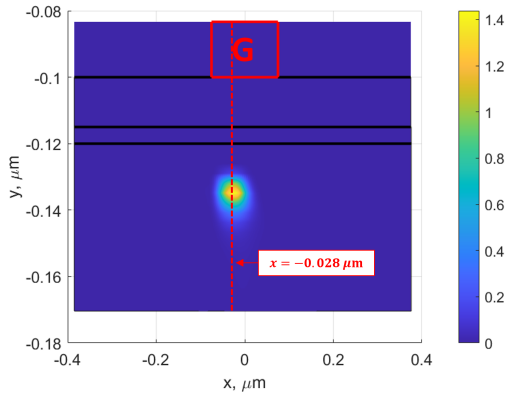

Fig. 5: Drain current local noise source at $f = 100$ Hz.

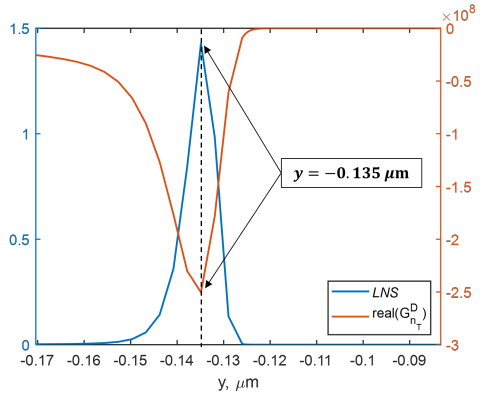

Fig. 6: Cross-section of real($\mathbf{G}^{(D)}_{n_T}(\mathbf{r}, f)$) and *LNS* along the y-axis extracted for $x = -0.028$ μm at $f = 100$ Hz.

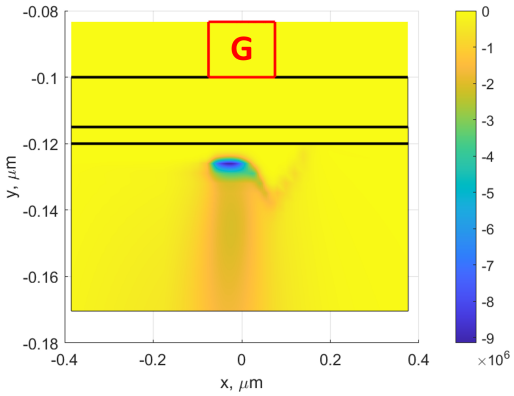

(a) Real part.

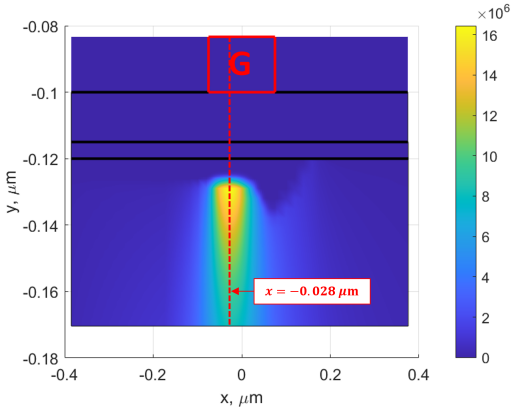

(b) Imaginary part.

Fig. 7: $\mathbf{G}^{(D)}_{n_T}(\mathbf{r}, f)$ at $f = 10$ kHz.

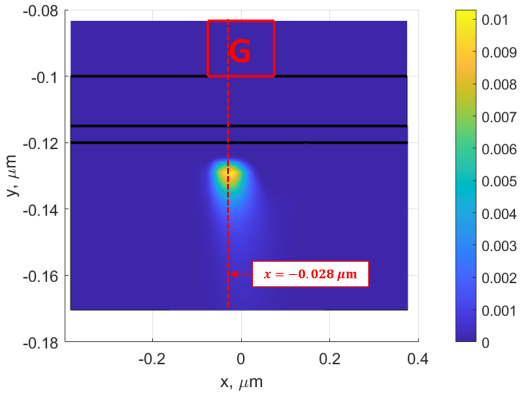

Fig. 8: Drain current local noise source at $f = 10$ kHz.

both the real and imaginary parts are shifted in depth into the buffer, extending under the gate contact and towards the source side. The real part presents a broad negative peak located at $y = -0.135$ μm, while the imaginary part shows a sharper positive peak at $y = -0.138$ μm and a wider negative region deeper into the buffer. Notice that the real part is much higher in absolute value with respect to the imaginary part, thus playing a predominant role in selecting the location of the overall local noise source. Fig. 5 shows the *LNS* with a marked positive peak under the gate contact, located deep in the buffer. A cross section of both the real part of $\mathbf{G}^{(D)}_{n_T}(\mathbf{r}, f)$ and *LNS* is taken at $x = -0.028$ μm, as shown by the red lines in Fig. 4a and Fig. 5. As shown in Fig. 6, both functions exhibit a peak at $y = -0.135$ μm, confirming that the GF real part yields the dominant contribution at this frequency.

At higher frequency, both the real and imaginary part of the trap rate equation GF extend under the gate contact, having the same order of magnitude, as shown in Fig. 7 for $f = 10$ kHz. Contrary to the low-frequency case, here the imaginary part yields the major contribution to the location of the *LNS*: the absolute value of its broad positive peak, located at $y = -0.128$ μm, is much smaller than the GF dominant contribution below the cut-off, making the overall drain noise decrease, as shown in Fig. 8. The *LNS* is characterized by a sharp positive peak under the gate contact, at the depth of $y = -0.128$ μm. The cross-sections of the GF imaginary part and *LNS*, extracted at $x = -0.028$ μm, are shown Fig. 9, showing a tight correlation in the peak location.

Despite the Lorentzian-like shape (see Fig. 2), drain and gate noise cannot be approximated by a simple single-pole spectrum. In fact, the dynamics is characterized by two char-

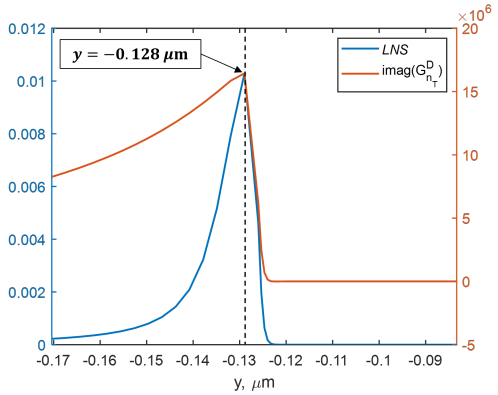

Fig. 9: Cross-section of imag($\mathbf{G}_{n_T}^{(D)}(\mathbf{r}, f)$) and *LNS* along the y-axis extracted for $x = -0.028$ μm at $f = 10$ kHz.

acteristic frequencies, more easily found by inspecting the drain-gate noise correlation spectrum and the imaginary part of the drain-gate element of the Y small-signal admittance matrix Y_{DG}. A statistical analysis is also helpful to correlate these two quantities, besides allowing for the device variability analysis. Here, we use a Gaussian distribution of the trap energy with variance equal to 10 meV (see inset of Fig. 10a), simulated with 30 samples. The statistical analysis shows that the imaginary part of the drain-gate current noise correlation and imag(Y_{DG}), reported in Fig. 10, present a negative peak at lower frequency and a positive peak at higher frequency. Similar correlation in the frequency trends is also found for other parameters, e.g., real part of the correlation spectrum and imag(Y_{DD}), i.e., the output admittance, not shown for brevity.

IV. Conclusions

We exploit an in-house TCAD simulator implementing the DD model coupled to the trap rate equations to investigate noise spectra and AC behavior in a GaN HEMT. The analysis is carried out with nominal trap parameters allowing for a deep insight into the local noise sources, and showing that the Green's functions identify the regions of the device where traps contribute to drain noise below (real part) or above (imaginary part) the noise cut-off. The trap dynamics induce though a detailled frequency trend which is not merely Lorentzian, as can be observed by drain-gate noise spectrum. Moreover, the statistical uncertainty of the trap parameter affects both the noise spectrum and Y parameters, which are found to be significantly correlated. The proposed analysis will aid at the interpretation of experimental noise and AC data, linking them to the internal trap distribution.

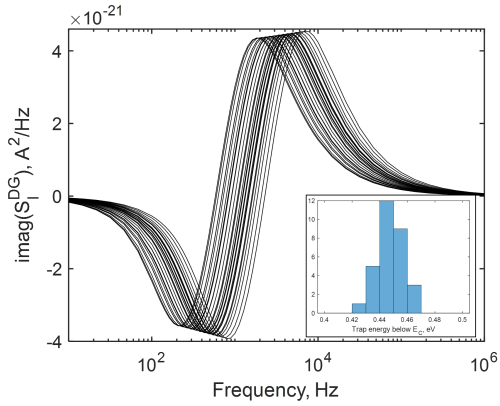

(a) Real part of the drain-gate correlation spectrum.

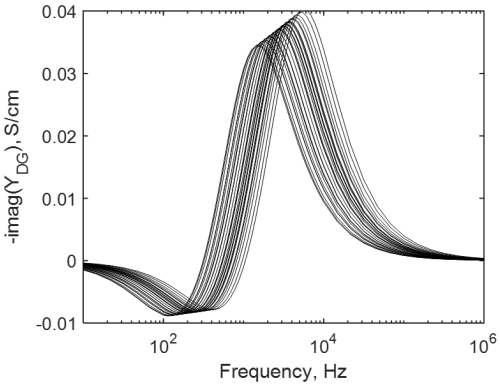

(b) Opposite of imaginary part of the drain-gate element of the HEMT AC Y matrix.

Fig. 10: Statistical distribution of the noise correlation and of the drain-gate AC parameter.

References

[1] U. Mishra, S. Likun, T. Kazior, and Y.-F. Wu, "GaN-based RF power devices and amplifiers," *Proceedings of the IEEE*, vol. 96, no. 2, pp. 287–305, feb 2008.

[2] G. Meneghesso, G. Verzellesi, F. Danesin, F. Rampazzo, F. Zanon, A. Tazzoli, M. Meneghini, and E. Zanoni, "Reliability of GaN high-electron-mobility transistors: State of the art and perspectives," *IEEE Transactions on Device and Materials Reliability*, vol. 8, no. 2, pp. 332–343, jun 2008.

[3] N. Zagni, G. Verzellesi, and A. Chini, "Temperature-independent current dispersion in 0.15 μm AlGaN/GaN HEMTs for 5g applications," *Micromachines*, vol. 13, no. 12, p. 2244, dec 2022.

[4] A. M. Angelotti, G. P. Gibiino, A. Santarelli, and C. Florian, "Experimental characterization of charge trapping dynamics in 100-nm AlN/GaN/AlGaN-on-si HEMTs by wideband transient measurements," *IEEE Transactions on Electron Devices*, vol. 67, no. 8, pp. 3069–3074, aug 2020.

[5] P. Beleniotis, F. Schnieder, S. Chevtchenko, and M. Rudolph, "Localization of trapping effects in GaN HEMTs with pulsed s-parameters and compact models," in *2022 17th European Microwave Integrated Circuits Conference (EuMIC)*. IEEE, sep 2022.

[6] P. V. Raja, N. K. Subramani, F. Gaillard, M. Bouslama, R. Sommet, and J.-C. Nallatamby, "Identification of buffer and surface traps in fe-doped AlGaN/GaN HEMTs using Y21 frequency dispersion properties," *Electronics*, vol. 10, no. 24, p. 3096, dec 2021.

[7] E. Catoggio, S. Donati Guerrieri, and F. Bonani, "TCAD modeling of GaN HEMT output admittance dispersion through trap rate equation Green's functions," *Electronics*, vol. 12, no. 11, p. 2457, may 2023.

[8] F. Bonani and G. Ghione, *Noise in Semiconductor Devices*. Springer Berlin Heidelberg, 2001.

[9] S. Donati Guerrieri, C. Ramella, F. Bonani, and G. Ghione, "Efficient sensitivity and variability analysis of nonlinear microwave stages through concurrent TCAD and EM modeling," *IEEE Journal on Multiscale and Multiphysics Computational Techniques*, vol. 4, pp. 356–363, 2019.

[10] S. Donati Guerrieri, M. Pirola, and F. Bonani, "Concurrent efficient evaluation of small-change parameters and green's functions for TCAD device noise and variability analysis," *IEEE Transactions on Electron Devices*, vol. 64, no. 3, pp. 1269–1275, mar 2017.